(NASA-CR-197994) GAMMA-RAY EMISSION FROM GLOBULAR CLUSTERS. SHOCK HIGH ENERGY EMISSION FROM THE BE-STAR/PULSAR SYSTEM PSR 1259-63. ECHOES IN X-RAY NOVAE Annual Status Report, 15 Apr. 1994 - 14 Apr. 1995 (Columbia Univ.) 16 p

N95-24381

Unclas

G3/93 0045337

NASA-CR-197994

CAL-2302

IN-93-CR
45337
P. 16

National Aeronautics and Space Administration

COMPTON GAMMA-RAY OBSERVATORY

ANNUAL STATUS REPORT FOR NAG 5-2235

Submitted to:

Dr. Jay Norris – Code 668.1
Laboratory for High Energy Astrophysics
Space Sciences Directorate
NASA/Goddard Space Flight Center
Greenbelt, MD 20771

Submitted by:

The Trustees of Columbia University
in the City of New York
Box 20, Low Memorial Library
New York, New York 10027

Prepared by:

Columbia Astrophysics Laboratory
Departments of Astronomy and Physics
Columbia University
538 West 120^{th} Street
New York, New York 10027

Principal Investigator:

Philip Kaaret
Assistant Professor of Physics

Titles of Research:

"Gamma-Ray Emission from Globular Clusters"; "Shock High Energy Emission from the Be-Star/Pulsar System PSR 1259-63"; and "Echoes in X-Ray Novae"

Period of Covered by Report: 15 April 1994 – 14 April 1995

April 1995

Annual Status Report for NASA Grant NAG 5-2235

Philip Kaaret (P.I.)

April 6th, 1995

This grant covers work on the Compton phase 3 investigation, "Shock High Energy Emission from the Be-Star/Pulsar System PSR 1259-63" and cycle 4 investigations "Diffuse Gamma-Ray Emission at High Latitudes" and "Echoes in X-Ray Novae". The grant provides partial support for Prof. Philip Kaaret (P.I.) and two graduate students, Andrew Chen and Eric Ford.

Work under the investigation "Diffuse Gamma-Ray Emission at High Latitudes" has lead to the publication of a paper describing gamma-ray emissivity variations in the northern galactic hemisphere scheduled for publication in the *Astrophysical Journal Letters* in June, 1995. Using archival EGRET data, we have found a large irregular region of enhanced gamma-ray emissivity at energies greater 100 MeV. This is the first observation of local structure in the gamma-ray emissivity. We are presently preparing a paper on results from the southern galactic hemisphere.

Work under the investigation "Echoes in X-Ray Novae" is proceeding with analysis of data from OSSE from the transient source GRO J1655-40. The outburst of this source last fall triggered this Target of Opportunity investigation. Mr. Ford and Dr. Kaaret visited the Naval Research Laboratory (NRL) and learned how to operate the IGORE data analysis environment. Analysis of the OSSE data is now being performed by remote login to the OSSE computers. Preliminary spectral analysis shows emission out to 600 keV and a pure power law spectrum with no evidence of an exponential cutoff. Publication of the results will be in collaboration with Dr. Kroeger of NRL.

Work is complete on the analysis of BATSE data from the Be-Star/Pulsar System PSR 1259-63. A paper describing these results is now in preparation.

A LOCALIZED EXCESS OF DIFFUSE GAMMA RADIATION

A. CHEN, J. DWYER, P. KAARET
Department of Physics and Columbia Astrophysics Laboratory
Columbia University, New York, NY 10027

Submitted to Astrophysical Journal Letters 1995 January 31

ABSTRACT

Using archival EGRET gamma-ray data and atomic hydrogen (H I) column densities derived from 21 cm radio observations, we have found a large irregular region in the northern galactic hemisphere extending from ($l \sim 90°$, $b \sim 52°$) to ($l \sim 45°$, $b \sim 77°$) with a significant enhancement in the gamma-ray emissivity compared to the surrounding sky. The region contains no previously identified gamma-ray point sources. The emission may arise from a localized enhancement in cosmic-ray density or from the presence of matter other than H I. If the emission is due to unseen matter, a column density enhancement equivalent to 2×10^{20} H-atoms cm^{-2} is required.

Subject headings: gamma radiation, cosmic rays, galactic structure

To appear in: Astrophysical Journal (Letters)

June 1995

1. INTRODUCTION

The gamma-ray sky in the energy range between 30 MeV and 10 GeV is dominated by diffuse emission resulting from the interaction of cosmic-rays with matter and radiation in our galaxy. The primary processes involved are gamma-ray production from the decay of neutral pions resulting from the interaction of cosmic-ray nuclei with interstellar gas, bremsstrahlung of cosmic-ray electrons (and positrons) on interstellar gas, and inverse-Compton scattering of cosmic-ray electrons with low energy photons. This basic picture of diffuse gamma-ray emission is supported by the positive correlation between interstellar gas column density and gamma-ray flux obtained with SAS-2 (Fichtel, Simpson, & Thompson 1978), COS-B (Bloemen, Blitz, & Hermsen 1984), and recently the EGRET instrument on CGRO (Hunter et al 1994).

This paper presents an analysis of diffuse gamma-ray emission at high galactic latitudes ($|b| > 30°$). Analysis of the diffuse emission at high latitudes has several advantages over low latitudes ($|b| < 20°$). The likelihood of coincidental superposition of features is greatly reduced. Most of the mass column density of interstellar gas is believed to be in the form of atomic hydrogen (Kulkarni & Heiles 1988), H I, which is well measured using 21 cm radio data (Dickey & Lockman 1990). Finally, the bulk of H I lies closer to the plane than the scale height of cosmic-rays, so the cosmic-ray density can be approximated as constant along each line of sight. These simplifications allow direct correlation of the gamma-ray emission with the H I column density to determine the gamma-ray emissivity from cosmic-ray interactions with atomic hydrogen.

This paper presents an analysis of the gamma-ray emissivity in the northern galactic hemisphere. We begin by considering the simplest reasonable model for the diffuse emission: an isotropic component and uniform emissivity. Examining the residuals from this model, we find that the largest deviations are due to a gamma-ray excess in a single contiguous region. We show that the excess gamma-ray intensity within this region is due to enhanced emissivity and present the emissivity energy spectrum. We conclude with a discussion of potential sources of the emissivity enhancement.

2. DATA

The gamma-ray data were obtained from the EGRET instrument (Fichtel et al. 1993). We used the archived maps of photon counts and exposure in 0.5° pixels and several energy bins. The files used were dated from 7 December 1994, and include the low energy exposure corrections (Thompson et al. 1993). We added the data from each viewing period from 22 April 1991 to 24 August 1993 to produce all-sky maps. To investigate the possibility of unusual instrument response or inaccurate exposure calculation near the edge of the field of view of EGRET, we repeated the analysis truncating the data from each viewing period to a 30° radius around the instrument axis and found no significant changes in the results discussed below. Gamma-ray point sources included in the first EGRET point source catalog (Fichtel et al. 1994) were removed by deleting a 15° diameter circle centered on each source.

The hydrogen column density is derived from the Bell Labs radio survey of 21 cm emission (Stark et al. 1992), which includes all emission within a velocity interval -360 to +360 km s^{-1} LSR and has an accuracy of 0.1 K (equivalent to 2×10^{17} H-atom cm^{-2}). Column densities were calculated with no opacity correction. The maximum opacity correction for a spin temperature $T_s > 150$ K is < 6%. The H I data were convolved to match the EGRET point spread function (Thompson et al. 1993) for the appropriate energy range. The H I column density for each field was weighted with the spatially varying gamma-ray exposure to allow direct comparison to the gamma-ray intensity.

3. RESULTS

The simplest reasonable model of diffuse gamma radiation consists of a uniform cosmic ray intensity and an isotropic extragalactic component. This model predicts a linear correlation between gamma-ray intensity and mass column density. Figure 1 shows the correlation between gamma-ray intensity J, for energies $E > 100$ MeV, and H I column density N_{HI} for the northern galactic hemisphere ($b > 30°$). Each point represents an integration over a distinct field approximately 5° by 5°. The errors in gamma-ray intensity are purely statistical. No error was assigned to the H I column densities. A least squares fit to the data of $J = I+qN_{HI}$ gives an average excess flux not correlated with H I of $I = 1.47{\pm}0.03{\times}10^{-5}$ photons cm^{-2} s^{-1} ster^{-1} and an average gamma-ray emissivity $q = 3.60{\pm}0.09{\times}10^{-26}$ photons s^{-1} ster^{-1} H-atom^{-1}. The quoted errors are purely statistical. The fit has $\chi^2_\nu = 2.0$. The non-statistical deviations from the fit are larger than expected from the estimated systematic errors in the H I data or the amount of H I expected outside the velocity range of the map. These deviations may be due to spatial variations in the H I emissivity or the distribution of matter other than H I.

The excess flux not correlated with H I is thought to be primarily extragalactic in origin (Fichtel, Simpson, & Thompson 1978) but may have a contribution from the halo of our galaxy. Due to the correlation between the slope and intercept values of the linear fit, spatial variations in the HI emissivity will influence the value obtained for the isotropic component. To estimate the uncertainty in the isotropic component, we have performed correlation fits of J versus N_{HI} using a variety of sky regions and field sizes. We find an isotropic flux $I = 1.5{\pm}0.3{\times}10^{-5}$ photons cm^{-2} s^{-1} ster^{-1} for gamma-ray energies $E > 100$ MeV, where the error includes systematic uncertainties. Our value for the isotropic flux is in agreement with the SAS-2 results (Fichtel, Simpson, & Thompson 1978) and with an analysis of EGRET data performed by Osborne, Wolfendale, & Zhang (1994). We note that we have performed no subtraction of the inverse-Compton component (Chi et al. 1989).

Once the value of the (assumed) isotropic component is fixed, it is possible to calculate the emissivity for each point on the sky. A map of the gamma-ray emissivity in the northern galactic hemisphere is shown in Figure 2. The emissivity was calculated as $q = (J-I)/N_{HI}$ using the value of the isotropic component I quoted above and the gamma-ray intensity for $E > 100$ MeV. To reduce the visual impact of statistical fluctuations, the gamma-ray intensity map was calculated from counts and exposure maps which had been smoothed by a $\sigma = 2°$ gaussian.

The figure can be interpreted, in two extreme cases, as a map of the cosmic-ray density or as a map of mass (normalized to the H I column density) other than H I. The average value of the emissivity is in agreement with the SAS-2 results for $|b| > 12.8°$ (Fichtel, Simpson, & Thompson 1978) and is significantly higher than more recent emissivity values obtained at lower latitudes (Hunter et al. 1994). An overall trend apparent in the map is that the emissivity is higher towards the galactic center and decreases towards the anticenter. This trend is in agreement with the results, at lower latitudes, of Strong et al. (1988), although our results show a steeper gradient. We note that the trend in our data could also arise from emission from a halo.

An extended irregular region of enhanced emissivity can be seen extending from roughly (l~90°, b~52°) to (l~45°, b~77°). For further analysis of this emissivity feature, we have defined the boundary show as an outline in Figure 2. This boundary was drawn to contain the contiguous areas with emissivity $q > 6\times10^{-26}$ photons s^{-1} $ster^{-1}$ H-atom^{-1}. The southern boundary of the region was defined to prevent confusion with known point sources; the emissivity excess appears to extend to lower latitudes. The emissivity within the feature is 1.6±0.1 times the average emissivity for $b > 30°$. We note that the feature persists at high significance if the isotropic background I, and therefore the calculated emissivity, is varied within our estimated systematic errors. This feature does not correspond to any previously identified gamma-ray source (Fichtel et al. 1994). However, three bright spots appear within the region. To investigate the possibility that these are point sources, we have performed a maximum likelihood analysis of the gamma-ray intensity using the LIKE procedure written by the EGRET team (Fichtel et al. 1993). For each of the bright spots in the feature, the best fit point sources were significant at the 3-4σ level and had confidence contours extending over several degrees. True point sources generally have more compact confidence contours. These results indicate that the emission is most likely diffuse. We note that no BL Lac or radio-loud quasars lie within the 1-σ confidence contours.

The gamma-ray excess may be due to the presence of mass other than H I that is uncorrelated with H I or due to an enhanced H I emissivity caused by either an increased cosmic-ray density or the presence of additional mass well correlated with H I. To attempt to distinguish between these possibilities, figure 3 shows the correlation between the gamma-ray intensity, for $E > 100$ MeV, and the H I column density for the region defined in Figure 2. The best fit linear correlation gives an average excess flux not correlated with H I $I = 1.1 \pm 0.2 \times 10^{-5}$ photons cm^{-2} s^{-1} ster^{-1}, consistent with our value for the northern galactic hemisphere ($b > 30°$). The emissivity for the region is $q = 8.5 \pm 1.6 \times 10^{-26}$ photons s^{-1} ster^{-1} H-atom^{-1}, which is larger than the northern sky emissivity at the level of 2.9 σ. We conclude that the gamma-ray excess is marginally more likely due to an enhancement in the H I emissivity than due to the presence of mass uncorrelated with H I. We note that the possibility that the feature is a chance fluctuation is excluded at the 6.5 σ level.

The energy spectrum of the emissivity of the region, as defined in Figure 2, is shown in Figure 4. The spectrum is adequately fit by a power law with a spectral index of -1.76±0.05. We have also fit the spectrum with a cosmic-ray emissivity model (Bertsch et al. 1993). The model uses near-earth measurements of the cosmic-ray spectra of electrons and protons, corrected for solar modulation, to predict the energy spectrum of gamma-ray emission. The intensity of the electron and proton cosmic ray components are the two free parameters of the model. This model produces a marginally worse fit than the simple power law. We note that for the spectrum of the entire sky for $b > 30°$, a power law fit is also marginally better than the cosmic-ray emissivity model. While comparison of the spectrum with gamma-ray production models would be useful in establishing the nature of the emission, the statistical quality of the data does not permit us to make firm statements. Additional gamma-ray data are required.

4. DISCUSSION

The next step in the study of this local region of enhanced gamma-ray emissivity will be to determine whether the excess radiation is due to an enhanced cosmic-ray density or the presence of excess matter. While obtaining improved gamma-ray data is important, observations at other wavelengths will be critical to either detect the excess mass or to characterize the mechanism of cosmic-ray enhancement.

The position of the region (l~90°) suggests that the emissivity enhancement is associated with the local spiral arm. For example, the feature may be due to the escape of cosmic-rays from the disk via a magnetic flux tube formed over a super bubble (Breitschwerdt & Schmutzler 1994) or it may result from inverse-Compton emission due to an enhanced low energy photon density over the spiral arm. Another possibility is that the feature is a region of cosmic ray acceleration; we note that there is a morphological coincidence between the edge of the feature near (l~90°, b~50°) and the density profile of high velocity gas, -100 to -150 km s^{-1} LSR . If the cosmic ray enhancement is contained within the ~200 pc scale height of the H I, then the feature is roughly 150 pc across. This is significantly smaller than the matter/cosmic-ray coupling lengths commonly found in the literature (Bertsch et al. 1993). However, compact regions of high cosmic-ray density within molecular clouds have already been observed (Bloemen et al. 1994).

If the gamma-ray enhancement is due to excess mass then the mass should be detectable at other wavelengths. Making the conservative assumption that the emissivity of the matter is the same as the average emissivity for H I for $b > 30°$, then column densities equivalent to $2\text{-}3\times10^{20}$ H-atoms cm^{-2} would be necessary to explain the gamma-ray excess. If the unseen matter is farther from the plane than the H I, where, presumably, the cosmic ray density is lower, more matter is required. Unfortunately, only limited data are available on the distribution of matter, other than H I, at high galactic latitudes.

Excess mass in the form of dust should be revealed by its infrared emission. We have searched for, and not found, correlation between the gamma-ray emissivity map and the IRAS 100 μm sky survey data. We note that the covering fraction of IR excess clouds is probably too low to explain the gamma radiation (Désert, Bazell, & Boulanger 1988).

No existing survey of molecular gas has adequate coverage over the region. Warm molecular gas would produce molecular line emission, and cold molecular gas may be detectable via absorption line measurements (Wilson & Mauersberger 1994). Detection of cold molecular gas would be of particular interest as it has been proposed that cold H_2

comprises a significant fraction of the dark matter in the outer galaxy (Lequeux, Allen, & Guilloteau 1993).

Ionized gas is detectable in the radio, optical, and x-ray bands. Radio dispersion measures of pulsars in globular clusters (Reynolds 1991) show ionized hydrogen (H II) to H I column density ratios as high as 0.64. The free electron model of Taylor and Cordes (1993) gives a value of 7×10^{19} H-atoms cm^{-2} in H II towards ($l\sim90°$, $b\sim50°$). However, this model contains little information on the spatial dependence of H II at high latitudes due to the paucity of pulsars with $b > 30°$. We note that no pulsar with an independently determined distance lies within our region of enhanced emissivity. The ionized components of the local bubble has been mapped with x-ray data and is too low to explain the gamma radiation (Juda et al. 1991). The best avenue for detection of ionized gas within this local region of enhanced gamma-ray emissivity is optical observations of the H_α recombination line. It is important that such observations be made.

We thank J. Mattox, D. Macomb, D. Kniffen, and T. McGlynn for assistance with the EGRET data. The H I survey data were obtained from the Astronomical Data Center and the National Space Science Data Center. This research was supported by grant NAG 5-2235 from the NASA Compton Observatory guest investigator program.

References

Berezinskii, V.S. et al. 1990, Astrophysics of Cosmic Rays, (Amsterdam: North-Holland).

Bertsch, D.L. et al. 1993, ApJ, 416, 587

Bloemen, J.B.G.M., Blitz, L., & Hermsen, W. 1984, ApJ, 279, 136

Bloemen, H. et al. 1994, A&A, 281, L5

Breitschwerdt, D. & Schmutzler, T. 1994, Nature, 371, 774

Chi, X. et al. 1989, J. Phys. G., 15, 1495

Désert, F.X., Bazell, D., & Boulanger, F. 1988, ApJ, 334, 815

Dickey, J.M. & Lockman, F.J. 1990, ARA&A, 28, 215

Fichtel, C.E. et al. 1993 in The Second Compton Symposium, ed. C.E. Fichtel, N. Gehrels, & J.P. Norris (AIP Conf. 304), 721

Fichtel, C.E. et al. 1994, ApJS, in press

Fichtel, C.E., Simpson, G.A., & Thompson, D.J. 1978, ApJ, 222, 833

Hunter, S.D. et al. 1994, ApJ, in press

Juda, M. et al. 1991, ApJ, 367, 182

Kulkarni, S.R. & Heiles, C. 1988, in Galactic and Extragalactic Radio Astronomy, ed. G.L. Verschuur & K.I. Kellermen, (Springer-Verlag, Berlin),

Lequeux, J., Allen, R.J., & Guilloteau, S. 1993, A&A, 280, L23

Osborne, J.L., Wolfendale, A.W., & Zhang, L. 1994, J. Phys. G, 20, 1089

Reynolds, R.J. 1991, ApJ, 372, L17

Stark, A.A. et al. 1992, ApJS, 79, 77

Strong, A.W. et al. 1988, A&A, 207, 1

Taylor, J.H., & Cordes, J.M. 1993, ApJ, 411, 674

Thompson, D.J. et al. 1993, ApJS, 86, 629

Wilson, T.L. & Mauersberger, R. 1994, A&A, 282, L41

Figure Captions

FIG. 1 The correlation between EGRET gamma-ray intensity for energies $E > 100$ MeV, J, and the atomic hydrogen column density, N_{HI}, for the northern galactic hemisphere ($b >$ 30°). Each point represents an integration of gamma-ray intensity and H I column density over a distinct field approximately 5° by 5° in size. The straight line is a least squares linear fit to the data.

FIG. 2 A map of the gamma-ray emissivity for energies $E > 100$ MeV for high galactic latitudes. The white outline indicates the boundaries of the region of enhanced emissivity described in the text. Known point sources have not been removed and are indicated by white circles of 15° diameter which is approximately three times the FWHM of the EGRET point spread function for $E > 100$ MeV.

FIG. 3 Gamma-ray intensity for energies $E > 100$ MeV versus H I column density for fields within the region of enhanced emissivity defined in fig. 2. The solid line is the best-fit linear correlation between intensity and H I column density. The line has an intercept $I = 1.1 \pm 0.2 \times 10^{-5}$ photons cm^{-2} s^{-1} ster^{-1} and a slope $q = 8.5 \pm 1.6 \times 10^{-26}$ photons s^{-1} ster^{-1} H-atom^{-1}. The best-fit linear correlation for the northern galactic sky ($b >$ 30°) is shown as a dotted line.

FIG. 4 The differential energy spectrum of the emissivity of the region of enhanced emissivity defined in figure 2. The solid line represents the best fit power law. The power law has a spectral index of -1.76±0.05 and the fit has $\chi^2_\nu = 1.9$. The dashed line is a fit to a two component cosmic-ray emissivity model in which the coefficients of the electron bremsstrahlung and the proton-induced components are free parameters. The best fit values of the coefficients are 3.8±0.3 and 3.3±0.4, respectively, and the fit has $\chi^2_\nu = 2.3$.

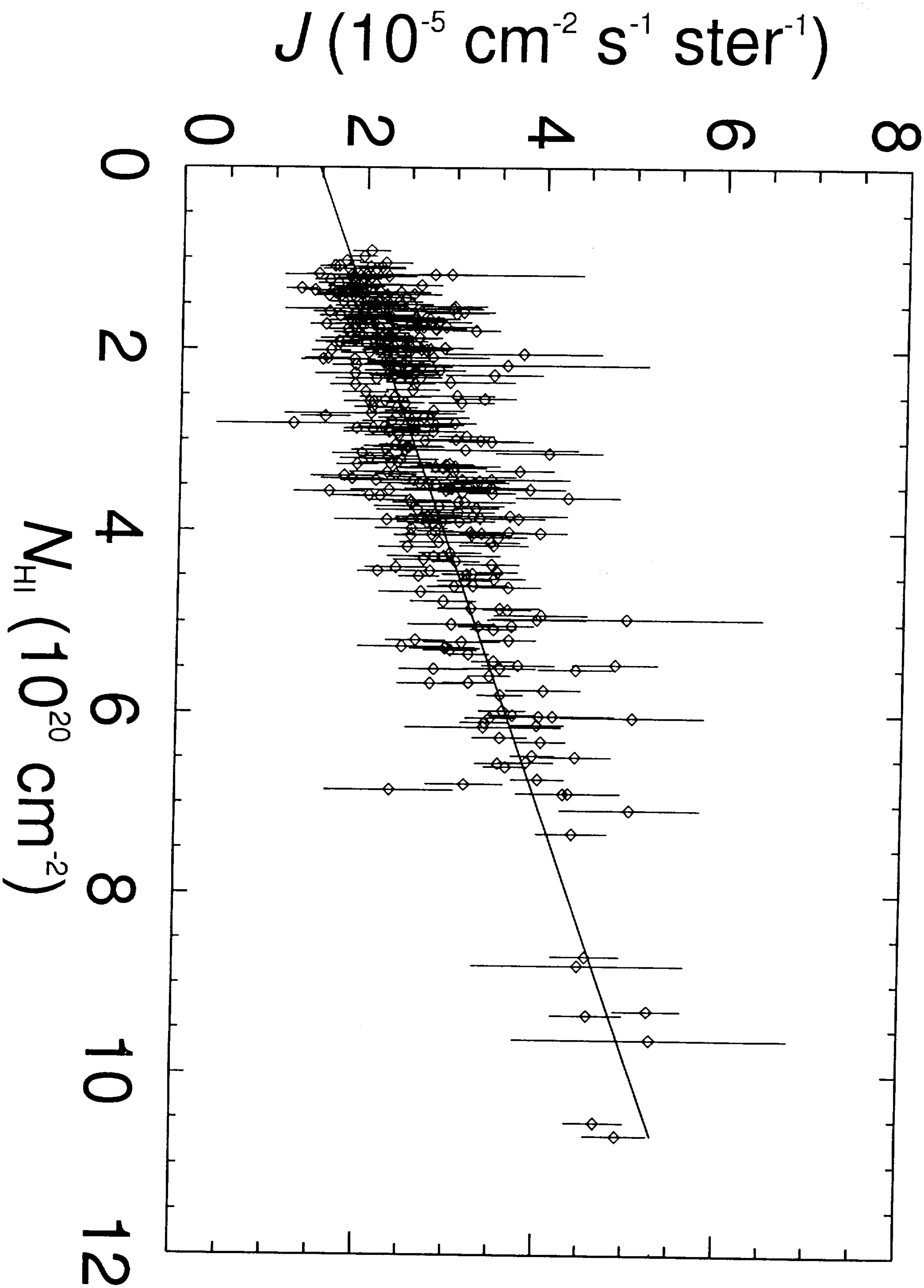

Figure 1

North Galactic Cap ($b > 30^\circ$)

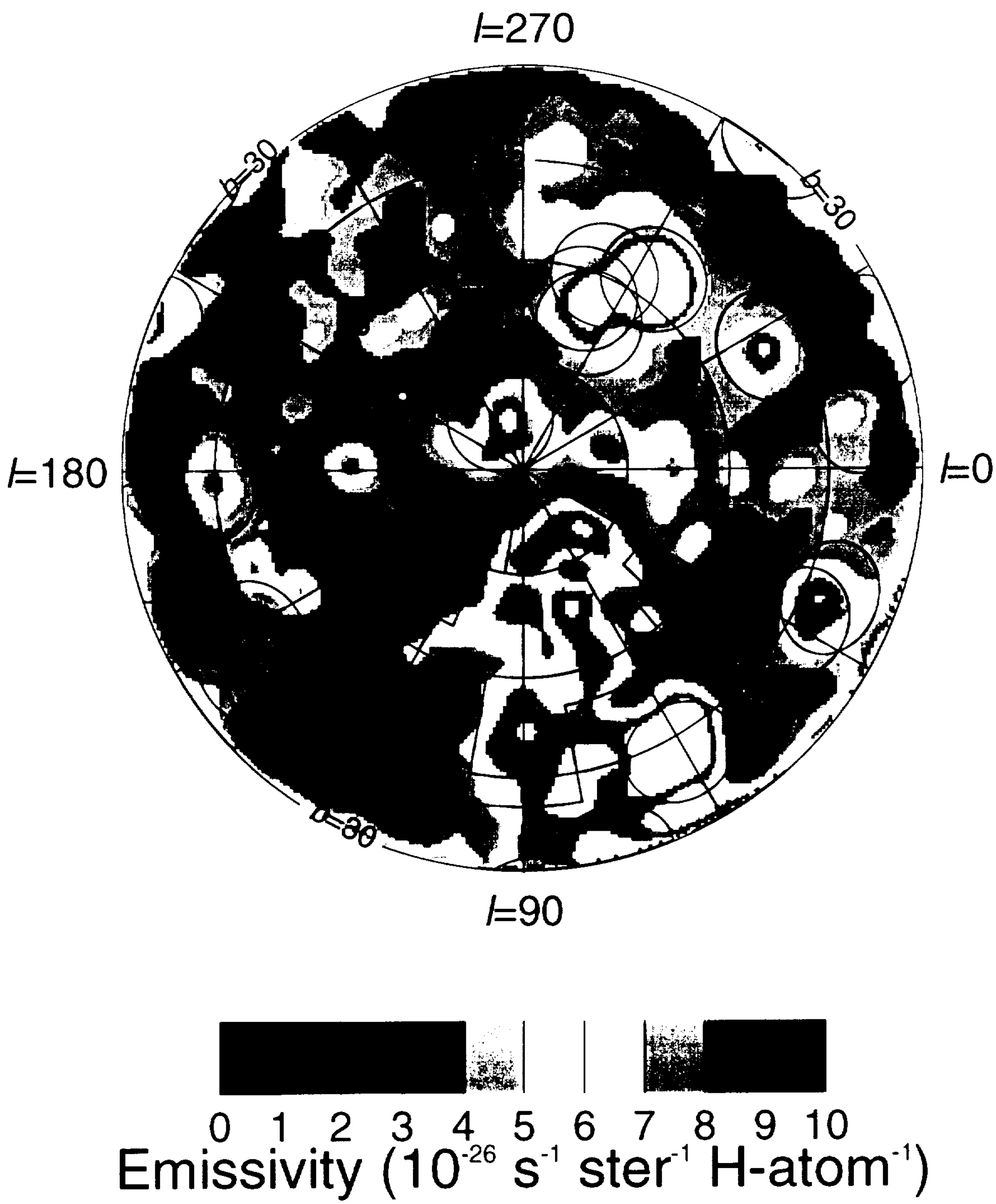

Figure 2

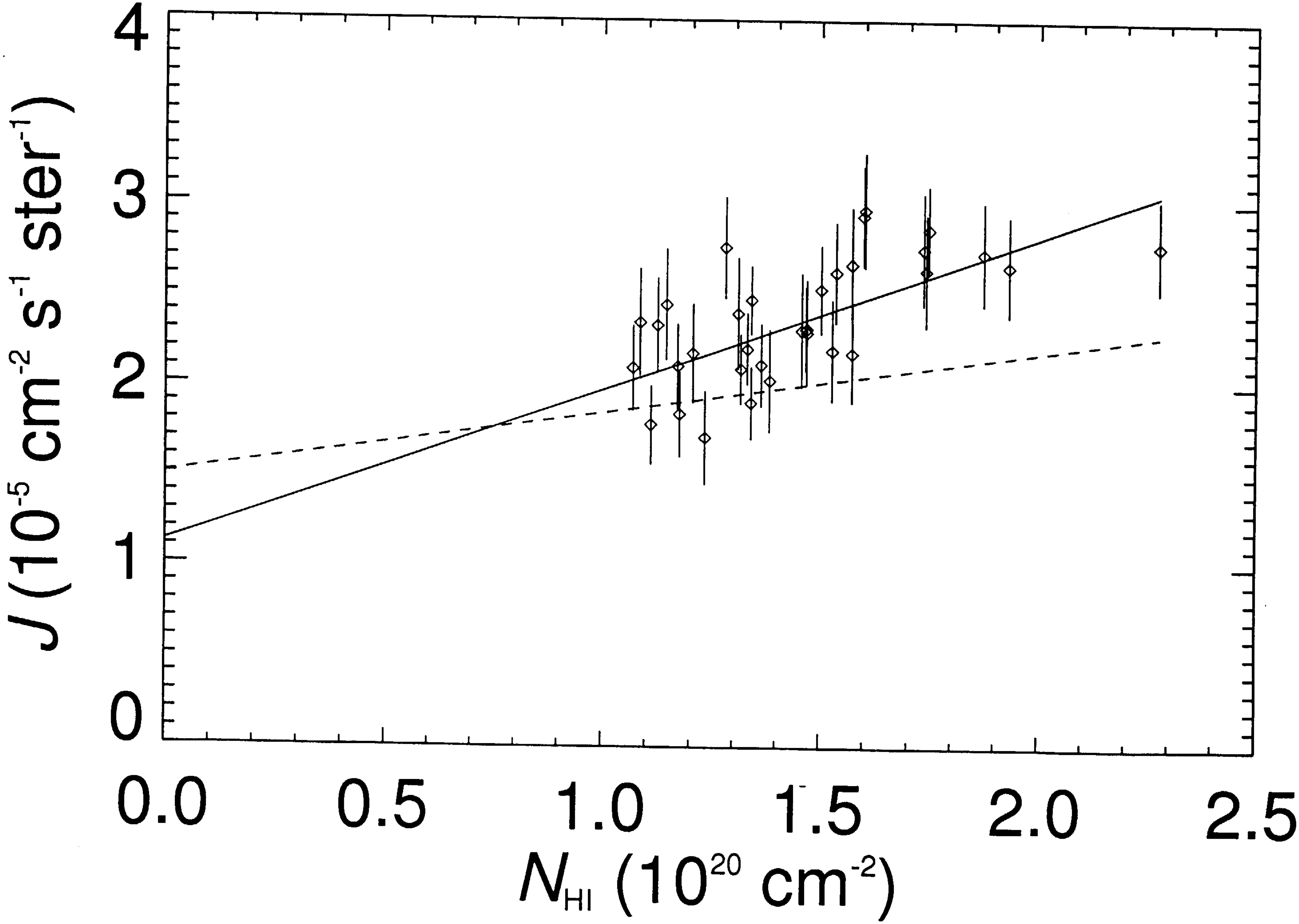

Figure 3

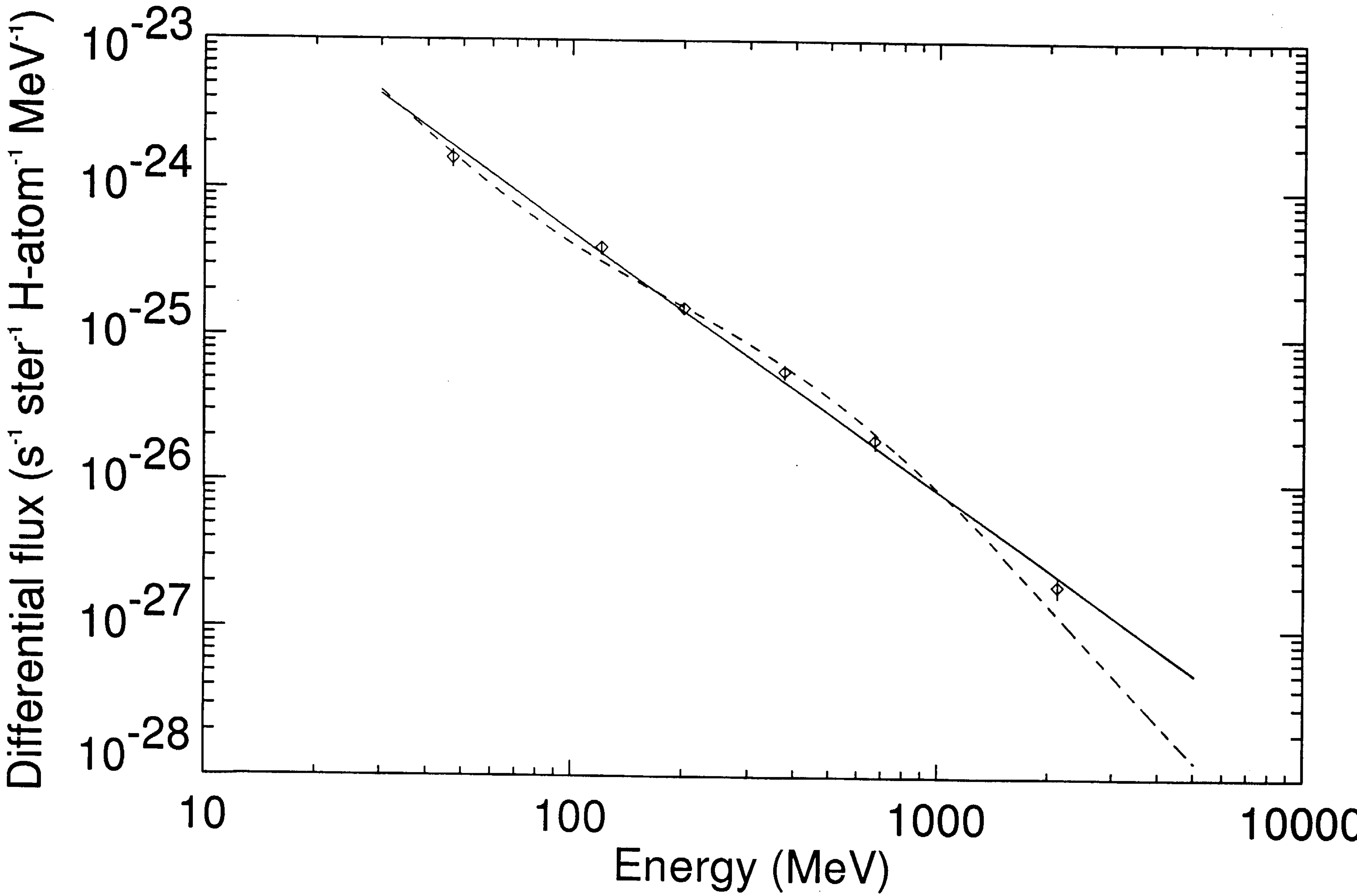

Differential flux (s-1 ster-1 H-atom-1 MeV-1)
10-23
10-24
10-25
10-26
10-27
10-28
10
100
1000
10000
Energy (MeV)

Figure 4